Published by IOP Publishing for Sissa Medialab

Received: *January 21, 2020*
Revised: *March 1, 2020*
Accepted: *March 13, 2020*
Published: *April 6, 2020*

2020 JINST 15 P04007

The resolution of the MIEZE setup on the longitudinal neutron resonance spin-echo spectrometer at CMRR

B. Liu,[1] **Z. Wang, Y. Wang, C. Huang and G. Sun**

Key Laboratory of Neutron Physics, and Institute of Nuclear Physics and Chemistry, China Academy of Engineering Physics (CAEP), P.O. Box 919-218, Mianyang City 621900, Sichuan Province, PR China

E-mail: liubenqiong@caep.cn

Abstract: A longitudinal neutron resonance spin echo (L-NRSE) spectrometer combined with a MIEZE (modulated intensity with zero effort) configuration will be constructed at the C33 beam port at China Mianyang Research Reactor (CMRR). In the MIEZE mode, the analyzer is placed in front of the sample, and between the sample and the detector there is no other optical device. The MIEZE signal is sensitive to the neutron path length differences from the sample to the detector. In this work, we have analytically studied the effects of sample geometry, detector thickness, and experimental setup on the resolution function.

Keywords: Instrumentation for neutron sources; Spectrometers

[1]Corresponding author.

https://doi.org/10.1088/1748-0221/15/04/P04007

Contents

2020 JINST 15 P04007

1 Introduction

Neutron scattering technique plays a significantly important role in the study of the dynamical properties in condensed matters, chemical and biological systems. Neutron spin echo (NSE) spectroscopy is an ideal method for quasi-elastic neutron scattering (QENS) [1, 2], and has the highest energy resolution of all neutron scattering methods, typically in the range of ~neV to ~ μeV [3, 4]. The basic idea of the neutron spin echo technique is to encode the information on energy transfers in neutron scattering events by the spin phase of the neutrons. It allows the decoupling of the energy resolution from monochromatizing the primary neutron beam; whereas triple-axis and time-of-flight (TOF) spectrometers always have the intensity loss problem.

Golub and Gähler [5] introduced an alternative NSE method, i.e., the neutron resonance spin echo (NRSE) technique, which uses resonance spin flippers (RSFs) [6] to take place of the two strong static magnetic fields to define the precession regions [7, 8]. For the transversal NRSE technique, by using pairs of identical RF flippers with opposite DC fields it is possible to reduce stray fields to negligible values [9]. It has been developed in some neutron facilities, e.g., MUSES [10] at LLB-Saclay in France, VIN ROSE at J-Parc/MLF [11] in Japan. IN22-ZETA [12] at Institut Laue Langevin (ILL) in France and TRISP [13, 14] at Heinz Maier-Leibnitz Zentrum (MLZ) in Germany are combined with triple-axes. The longitudinal NRSE technique has been proposed for the spectrometer RESPECT at the European Spallation Source (ESS) in Sweden [15], and it has already been available at RESEDA [16, 17] at MLZ.

As NSE technique uses polarized neutrons, it is inherently sensitive to the depolarization of the neutron beam. Therefore, it can be quite challenging to perform experiments with external magnetic fields or ferromagnets and protonated materials. Then the technique of Modulation of IntEnsity with Zero Effort (MIEZE) has been developed [18], which employs one pair of resonance coils rather than two pairs in standard NRSE spectrometer. By operating the RSF at different frequencies, one can obtain an intensity modulated signal at the detector and the neutron energy

transfer during the scattering process at the sample is encoded in the contrast. The contrast denotes the ratio of the amplitude to the mean value of the intensity, and corresponds to the polarization in a conventional NSE instrument. Since all spin manipulations are performed before the sample, MIEZE is independent of depolarisation effects.

A lot of MIEZE tests have been performed [19, 20], and this technique has already been implemented at RESEDA and MIRA [21, 22] at MLZ, PF2/VCN [23] at ILL, VIN ROSE [11], and also the Larmor instrument at ISIS [24]. It has been demonstrated that it can be used under applied magnetic fields (e.g., 17 T at RESEDA [25]), and it also supports the studies of magnetic materials [26–28] and incoherent scatterers [19, 29, 30]. In this work, we firstly give a brief introduction about the longitudinal neutron resonance spin echo spectrometer combined with a MIEZE configuration under construction in the C33 port at CMRR. Then we present the study of the resolution function of the MIEZE spectrometer by an analytical method.

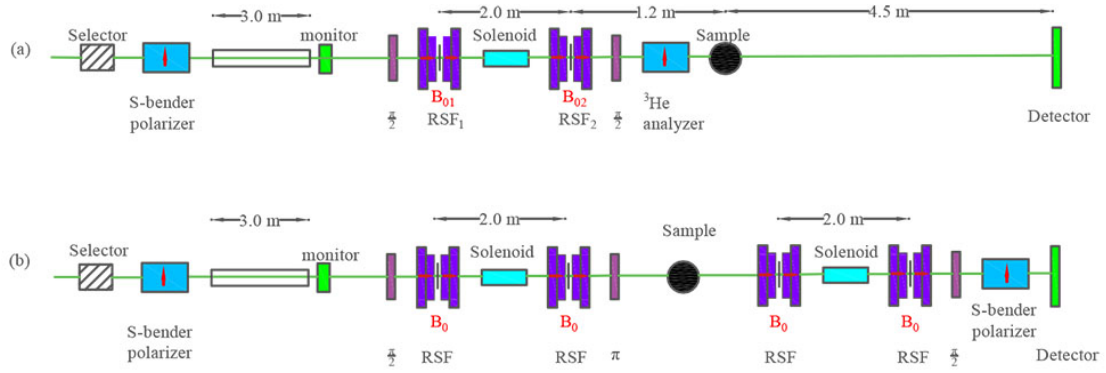

Figure 1. The schematic drawing of the longitudinal neutron spin echo spectrometer combined with a MIEZE configuration: (a) the MIEZE, and (b) NRSE option.

2 The MIEZE technique

A longitudinal neutron resonance spin echo spectrometer combined with a MIEZE geometry is under construction in the C33 port at CMRR. The size of the neutron beam is 30 mm×30 mm. Figure 1 shows the schematic layout of the instrument. The resonance spin flippers include a static magnetic field B_{0i} ($i = 1, 2$) and a radio frequency field B_i with frequency ω_i which induce neutron spin precessions. The static field B_{0i} is parallel to the neutron flight path, the RF field B_i is transverse to B_{0i} and the neutron beam. The distance between the first pair of resonance spin flippers is $L_1 = 2$ m, the distance between the second resonance spin flipper to the sample is $L_{2S} = 1.2$ m. For the MIEZE option, it is possible to perform measurements for sample-detector distance L_{SD} between 0.5 m and 5 m. A 2-dimensional position sensitive CASCADE detector [31] will be used, with ns time-resolution, and the active area is 20 cm×20 cm.

The two RF coils are operating at different frequencies in the range of 40 kHz $< \omega_{1,2} <$ 2 MHz. The Larmor conditions $\omega_{1,2} = \gamma B_{1,2}$ are satisfied for both of them, with $\gamma = 2\pi \cdot 2.912$ kHz/G. Downstream of the second RF coil, the neutron procession angle ψ can be written as

$$\psi = 2(\omega_2 - \omega_1)t_1 + 2\omega_2 L_1/v. \tag{2.1}$$

2020 JINST 15 P04007

One can find that ψ depends on the neutron velocity v and the time of arrival at the first RF coil t_1. At a certain position D, separated by L_2 from the second RF coil, the time of arrival of neutrons is given by

$$t_D = t_1 + \frac{L_1 + L_2}{v}, \tag{2.2}$$

and the corresponding neutron precession angle in eq. (2.1) can be written as

$$\psi_D = 2\left(\omega_2 - \omega_1\right)\left(t_D - \frac{L_1 + L_2}{v}\right) + 2\omega_2 L_1/v, \tag{2.3}$$

which is independent of the neutron velocity v on the condition:

$$(\omega_2 - \omega_1)(L_1 + L_2) = \omega_2 L_1, \tag{2.4}$$

and one gets $\psi_D = 2(\omega_2 - \omega_1)t_D$.

By employing a polarizer, a sinusoidal intensity modulation can be obtained. With a transmission probability $T = 0.5(\cos\psi_D + 1)$, one can obtain a pure sinusoidal intensity $I(t_D)$ with maximum contrast $C = 1$:

$$I(t_D)/I_0 = T = \frac{1}{2}[\cos 2(\omega_2 - \omega_1)t_D + 1]. \tag{2.5}$$

Assume that the scattering properties of the sample can be given by a scattering law $S(\omega)$ which is symmetric around zero-energy transfer with $\hbar\omega \ll 1/2mv^2$, where m is the neutron mass. The contrast at the detector position D can be written as [32]

$$I\left(t_D\right) = \frac{I_0}{2}\left[1 + \cos 2\left(\omega_2 - \omega_1\right)t_D\right]\int \cos\left[2\left(\omega_2 - \omega_1\right)\frac{\hbar\omega L_{SD}}{mv^3}\right] S\left(\omega\right)\mathrm{d}\omega, \tag{2.6}$$

where the scattering law $S(\omega)$ describes the scattering properties. The MIEZE time τ_{M} is defined as

$$\tau_M = \omega_M \frac{\hbar L_{SD}}{mv^3}, \tag{2.7}$$

which is equivalent to the spin echo time in NSE and NRSE instruments, with $\omega_M = 2(\omega_2 - \omega_1)$ called the modulation (or MIEZE) angular frequency. The role of the polarisation in NSE and NRSE measurements is taken by the cos-Fourier transform of $S(\omega)$ or the contrast C as

$$C = \int S(\omega)\cos(\omega\tau_M)\mathrm{d}\omega. \tag{2.8}$$

For cold neutrons with long wavelength, one can perform very high resolution measurements, since the energy resolution is proportional to the third power of neutron wavelength.

3 Path length differences due to a cylinder sample

The MIEZE method is related to time of flight method and it is quite sensitive to the path length differences ΔL_2 through the setup. The contrast of the MIEZE signal is reduced by several factors,

2020 JINST 15 P04007

such as the sample geometry, the resolution of the detector, the finite efficiency of the polarizer and analyzer. For simplification, here the contrast $C(q,\tau)$ can be written as [33]

$$C(q,\tau) = R \cdot \frac{S(q,\tau)}{S(q,0)}, \tag{3.1}$$

with the total reduction factor

$$R = R_{\text{coil}} \cdot R_{\text{detector}} \cdot R_{\text{sample}}, \tag{3.2}$$

where R_{coil} denotes the contrast reduction in the coil systems in front of the beam. It has no analytical form and can be mainly determined by the performance of the RF-spin flippers. With the longitudinal field geometry for the RF-spin flippers, this factor could be assumed to be close to 1 in the experimental limit [34]. R_{detector} describes the contrast reduction because of the thickness of the detector. These two factors only depend on the instrumental parameters, while R_{sample} depends on the geometries of both the experimental setup and the given sample. It can be determined by using Monte Carlo simulations as reported by Hayashida et al. [35] or by analytical calculations like in refs. [33, 36].

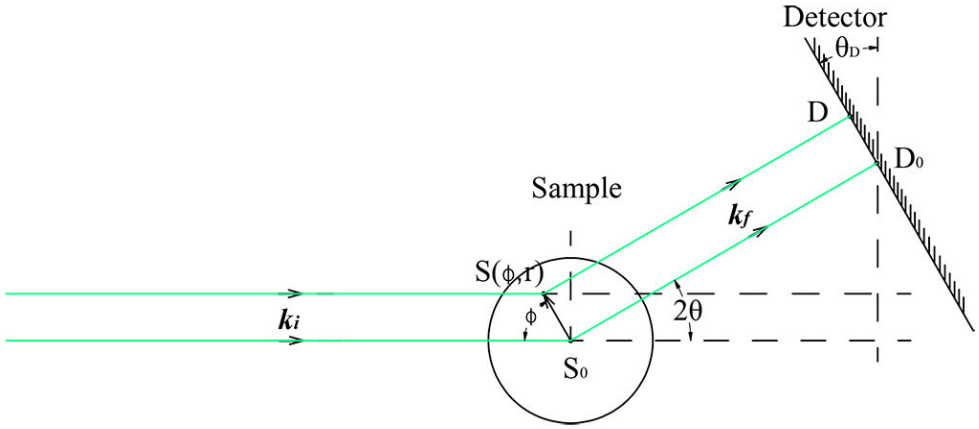

Figure 2. The scattering geometry in a cylinder sample with the radius r_0.

For simplicity we consider a cylinder sample with radius r_0 as depicted in figure 2, in the case of a parallel incoming beam the path length difference ΔL_2 can be written as

$$\Delta L_2 = \frac{r\cos\phi(\cos 2\theta - 1)}{\cos 2\theta} + \frac{r\sin\theta_D(\tan 2\theta\cos\phi + \sin\phi)}{\cos(2\theta - \theta_D)}, \tag{3.3}$$

with $S(r,\phi)$ an arbitrary scattering point respect to the centre of the sample, θ_D the tilt of the detector, and 2θ the scattering angle with $\theta = \arcsin(\frac{q\lambda}{4\pi})$ for a neutron wavelength λ and a momentum transfer q. The phase difference at the detector can be given by

$$\Delta\psi = 2\pi\frac{\Delta L_2}{\Lambda}, \tag{3.4}$$

where $\Lambda = 2\pi v/\omega_M$ is the distance passed by a neutron of velocity v over a period $2\pi/\omega_M$ of the oscillating signal [33].

The reduction factor can be obtained as

$$R_{\text{sample}} = \frac{1}{\pi r_0^2}\int_0^{2\pi}\int_0^{r_0}\cos\left(\frac{2\pi}{\Lambda}\Delta L_2\right) r\,\mathrm{d}r\mathrm{d}\phi. \tag{3.5}$$

2020 JINST 15 P04007

4 Path length differences due to a cuboid sample

Considering a cuboid sample with the width y_0 and thickness x_0, the path length difference ΔL_2 can be written as

$$\Delta L_2 = x + \frac{y \sin\theta_D - x\cos\theta_D}{\cos(\theta_D - 2\theta)}, \tag{4.1}$$

where $S(x,y)$ denotes the sample position. The reduction factor can be then obtained by averaging $\cos(\Delta\psi)$ over all the sample as follows

$$\begin{aligned} R_{\text{sample}} &= \frac{1}{x_0 y_0}\int_{-x_0/2}^{x_0/2}\int_{-y_0/2}^{y_0/2}\cos\left(\frac{2\pi\Delta L_2}{\Lambda}\right)\mathrm{d}y\mathrm{d}x \\ &= \mathrm{sin\,c}\left[\frac{\pi y_0 \sin\theta_D}{\Lambda\cos(\theta_D - 2\theta)}\right]\mathrm{sin\,c}\left\{\frac{\pi x_0[\cos(\theta_D - 2\theta) - \cos\theta_D]}{\Lambda\cos(\theta_D - 2\theta)}\right\}. \end{aligned} \tag{4.2}$$

In additions, the finite thickness of the detector ε_0 can also lead to the path length difference as follows,

$$\Delta L_2 = \frac{\varepsilon}{\cos(2\theta - \theta_D)}, \tag{4.3}$$

where ε is the depth of a given point in the detector. Assuming that the detection probability across the detector thickness doesn't change, the corresponding reduction factor can be written as

$$\begin{aligned} R_{\text{detector}} &= \frac{1}{\varepsilon_0}\int_{-\varepsilon_0/2}^{\varepsilon_0/2}\cos\left(\frac{2\pi\Delta L_2}{\Lambda}\right)\mathrm{d}\varepsilon \\ &= \mathrm{sinc}\left[\frac{\varepsilon_0\pi}{\Lambda\cos(2\theta - \theta_D)}\right]. \end{aligned} \tag{4.4}$$

In the CASCADE detector, boron coated foils are used to convert the neutrons and record the MIEZE signal. Each neutron detection plane is about 1 µm thick, and the detector thickness may be not a major factor of the contrast decreasing according to the requirement $\varepsilon_0 \ll 2\pi v/\omega_M$ for low frequency ω_{M}. However, for high Fourier times, the spin echo group is in the order of minimeter and only visible on one foil, reducing the efficiency of the detector as shown in [37].

5 Performance of a MIEZE setup

It has been demonstrated that the MIEZE technique is well adapted for the small-angle neutron scattering (SANS) configuration [33] as well as reflectometry [19, 38].

In order to estimate the accessible (q, τ)-range for a quasi-elastic experiment using the MIEZE option, the total reduction factor R has been calculated with the assumption $R_{\text{coil}} = 1$ in the two-arms (TA) and SANS methods as shown in figure 3. Figure 4 shows the accessible (q, τ)-range for a cuboid sample with the neutron wavelengths $\lambda = 4\,\text{Å}$ (where one can obtain the maximum flux), and $\lambda = 12\,\text{Å}$, respectively. The corresponding technical limits $\tau_{\text{M}} = 1.9\,\text{ns}$ and $\tau_{\text{M}} = 52\,\text{ns}$ are obtained with $L_1 = 2\,\text{m}$, $L_{2\text{S}} = 1.2\,\text{m}$, and $L_{\text{SD}} = 4.5\,\text{m}$. One can find that in a large q-range, the SANS configuration shows better performance than the TA mode. However, in the case that the cuboid sample is tilted by an angle with respect to the y-axis, one could also maximize the reduction factor R_{sample} by properly tilting the detector.

2020 JINST 15 P04007

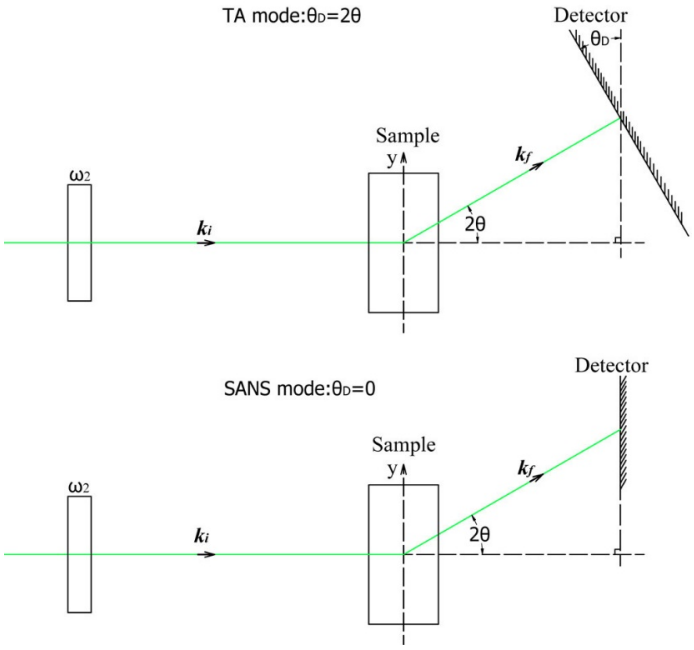

Figure 3. The two-arms mode and small-angle neutron scattering configuration, with the cuboid sample surface perpendicular to the incoming beam.

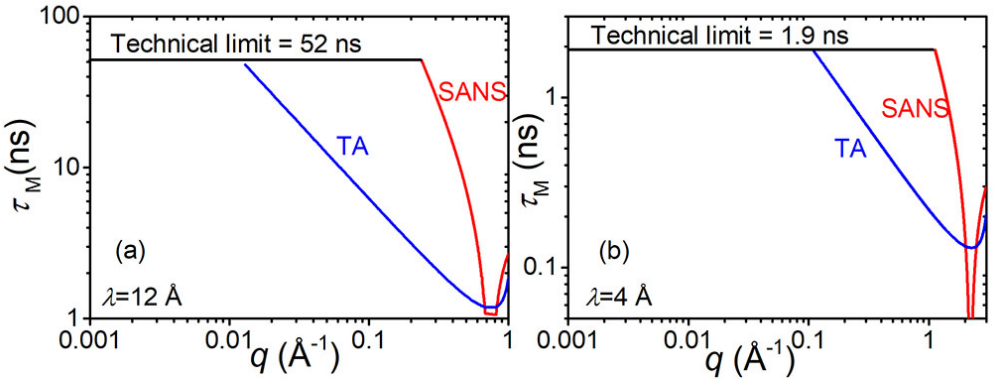

Figure 4. Accessible (q,τ)-range for (a) $\lambda = 12\,\text{Å}$, and (b) $\lambda = 4\,\text{Å}$, with the distance between the sample and detector $L_{\text{SD}} = 4.5\,\text{m}$, a detector thickness $\varepsilon_0 = 6\,\mu\text{m}$, and the cuboid sample size of 10×2 (width×thickness) mm^2.

In order to compare the effect of different sample geometries for measurement, the reduction factor R_{sample} has been plotted versus q for a cuboid sample and a cylinder sample in figure 5. It is obvious that different sample shapes show large differences, especially at larger q values.

According to eq. (2.7), the Fourier time is proportional to the oscillating magnetic field frequency of the RF. In figure 6, the effect of ω_{M} ranges from $2\pi\cdot$ 40 kHz to $2\pi\cdot$ 2 MHz has been simulated for a cuboid sample.

2020 JINST 15 P04007

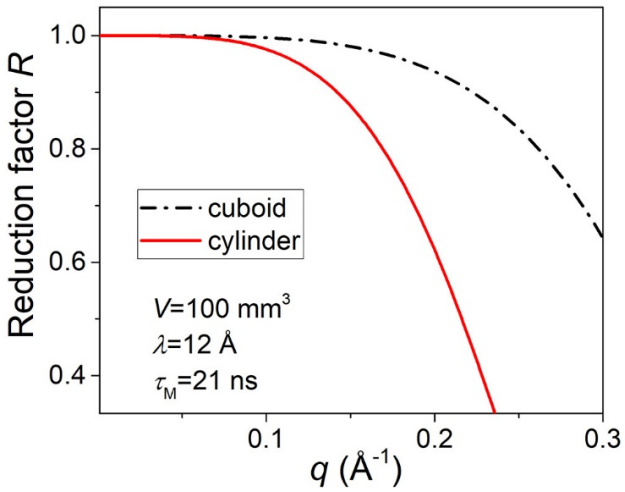

Figure 5. The reduction factor R versus q for a SANS configuration with different sample geometries, i.e., cylinder $r_0 = 3$ mm (red solid line) and cuboid 10×2 (width×thickness) mm^2 (black dash-dotted line), with $\lambda = 12$ Å, a detector thickness $\varepsilon_0 = 6$ µm. Both samples have the same volume $V = 100$ mm^3.

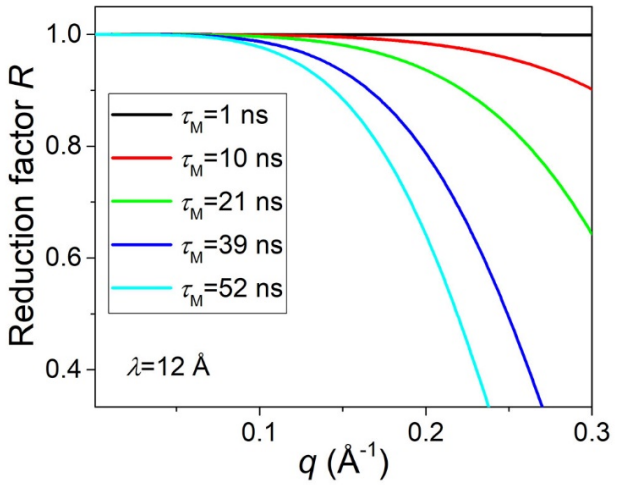

Figure 6. The reduction factor R versus q for a SANS configuration, with $\lambda = 12$ Å, the sample size of 10×2 (width×thickness) mm^2, and a detector thickness $\varepsilon_0 = 6$ µm. ω_M ranges from $2\pi \cdot 40$ kHz to $2\pi \cdot 2$ MHz, yielding a MIEZE time τ_M from 1 ns to 52 ns, respectively.

6 Conclusion

The MIEZE technique allows to perform low background quasi-elastic neutron scattering experiments in strong magnetic fields and depolarising samples because all beam manipulations are performed before the sample. However, it is quite sensitive to the neutron path difference ΔL_2 due to the instrumental setup and the sample geometry. We have discussed the major influence of ΔL_2 on contrast reduction of MIEZE measurements.

2020 JINST 15 P04007

Acknowledgments

This work is supported by the National Natural Science Foundation of China (Grant No. 11875238, No. U1830205), Science Challenge Project (Grant No. TZ2016004), the Key Laboratory of Neutron Physics CAEP (Grant No. 2017AB03), and National Key Research and Development Program of China (2017YFA0403703). We wish to thank Dr. N. Martin and Dr. C. Franz for helpful discussions and support.

References

[1] F. Mezei, *Neutron spin echo: a new concept in polarized thermal neuron techniques*, *Z. Phys.* **255** (1972) 146.

[2] F. Mezei, *Neutron Spin Echo*, Springer-Verlag, Berlin Heidelberg GmbH (1979).

[3] P. Schleger et al., *The long-wavelength neutron spin-echo spectrometer IN15 at the Institut Laue-Langevin*, *Physica* **B 241–243** (1997) 164.

[4] O. Holderer and O. Ivanova, *J-NSE: Neutron spin echo spectrometer*, *JLSRF* **1** (2015) A11.

[5] R. Golub and R. Gähler, *A neutron resonance spin echo spectrometer for quasi-elastic and inelastic scattering*, *Phys. Lett.* **A 123** (1987) 43.

[6] M. Köppe, P. Hank, J. Wuttke, W. Petry, R. Gähler and R. Kahn, *Performance and future of a neutron resonance spinecho spectrometer*, *J. Neutron Res.* **4** (1996) 261.

[7] T. Keller, R. Golub, F. Mezei and R. Gähler, *Recent developments and results from the neutron resonance spin-echo spectrometer (NRSE) at BENSC Berlin*, *Physica B Condens. Matter* **234–236** (1997) 1126.

[8] T. Keller, R. Golub, F. Mezei and R. Gähler, *A neutron resonance spin-echo spectrometer (NRSE) with tiltable fields*, *Physica B Condens. Matter* **241–243** (1997) 101.

[9] R. Gähler and R. Golub, *Neutron resonance spin echo, bootstrap method for increasing the effective magnetic field*, *J. Phys. (France)* **49** (1988) 1195.

[10] S. Longeville, *La spectroscopie neutronique à écho de spin à champ nul ou par résonance*, *J. Phys. IV France* **10** (2000) 59.

[11] H. Endo, T. Oda, M. Hino and T. Hosobata, *Current status of the neutron resonance spin echo spectrometer on BL06 "VIN ROSE" at MLF, J-PARC*, *Physica B Condens. Matter* **564** (2019) 91.

[12] S. Klimko et al., *Implementation of a zero-field spin-echo option at the three-axis spectrometer IN3 (ILL, Grenoble) and first application for measurements of phonon line widths in superfluid* ^{4}*He*, *Physica* **B 335** (2003) 188.

[13] T. Keller, K. Habicht, H. Klann, M. Ohl, H. Schneider and B. Keimer, *The NRSE-TAS spectrometer at the FRM-2*, *Appl. Phys.* **A 74** (2002) S332.

[14] T. Keller et al., *Scientific review: The triple axis spin-echo spectrometer TRISP at the FRM II*, *Neutron News* **18** (2007) 16.

[15] R. Georgii, J. Kindervater, C. Pfleiderer and P. Böni, *RESPECT: Neutron resonance spin-echo spectrometer for extreme studies*, *Nucl. Instrum. Meth.* **A 837** (2016) 123.

[16] C. Franz and T. Schröder, *RESEDA: Resonance spin echo spectrometer*, *JLSRF* **1** (2015) A14.

[17] C. Franz et al., *The longitudinal neutron resonant spin echo spectrometer RESEDA*, *Nucl. Instrum. Meth.* **A 939** (2019) 22.

2020 JINST 15 P04007

[18] R. Gähler, R. Golub and T. Keller, *Neutron resonance spin echo — a new tool for high resolution spectroscopy*, *Physica B Condens. Matter* **180-181** (1992) 899.

[19] W. Besenböck et al., *First scattering experiment on MIEZE: A fourier transform time-of-flight spectrometer using resonance coils*, *J. Neutron Res.* **7** (1998) 65.

[20] M. Bleuel et al., *First tests of a MIEZE (modulated intensity by Zero effort)-type instrument on a pulsed neutron source*, *Physica* **B 371** (2006) 297.

[21] R. Georgii, P. Böni, M. Janoschek, C. Schanzer and S. Valloppilly, *MIRA-A flexible instrument for VCN*, *Physica* **B 397** (2007) 150.

[22] R. Georgii et al., *Turn-key module for neutron scattering with sub-micro-eV resolution*, *Appl. Phys. Lett.* **98** (2011) 073505.

[23] T. Oda, M. Hino, M. Kitaguchi, H. Filter, P. Geltenbort and Y. Kawabata, *Towards a high-resolution TOF-MIEZE spectrometer with very cold neutrons*, *Nucl. Instrum. Meth.* **A 860** (2017) 35.

[24] N. Geerits et al., *Time of flight modulation of intensity by zero effort on Larmor*, *Rev. Sci. Instrum.* **90** (2019) 125101.

[25] J. Kindervater et al., *Neutron spin echo spectroscopy under 17 T magnetic field at RESEDA*, *EPJ Web Conf.* **83** (2015) 03008.

[26] S. Säubert, J. Kindervater, F. Haslbeck, C. Franz, M. Skoulatos and P. Böni, *Dipolar interactions in fe: A study with the neutron larmor precession technique MIEZE in a longitudinal field configuration*, *Phys. Rev.* **B 99** (2019) 184423.

[27] H. Hayashida, M. Hino, M. Kitaguchi, N. Achiwa and Y. Kawabata, *A new MIEZE technique for investigating relaxation of magnetic nanoparticles*, *Nucl. Instrum. Meth.* **A 600** (2009) 56.

[28] F. Haslbeck et al., *Ultrahigh-resolution neutron spectroscopy of low-energy spin dynamics in UGe_2*, *Phys. Rev.* **B 99** (2019) 014429.

[29] P. Hank, W. Besenböck, R. Gähler and M. Köppe, *Zero-field neutron spin echo techniques for incoherent scattering*, *Physica B Condens. Matter* **234–236** (1997) 1130.

[30] W. Häußler and L. Kredler, *Dynamic neutron scattering on incoherent system using efficient resonance spin flip techniques*, *AIP Conf. Proc.* **1599** (2014) 298.

[31] M. Köhli et al., *Efficiency and spatial resolution of the CASCADE thermal neutron detector*, *Nucl. Instrum. Meth.* **A 828** (2016) 242.

[32] F. Mezei, C. Pappas and T. Gutberlet, *Neutron spin echo spectroscopy: basics, trends and applications*, Springer-Verlag, Berlin Heidelberg, Germany (2003).

[33] G. Brandl, R. Georgii, W. Häußler, S. Mühlbauer and P. Böni, *Large scales-long times: Adding high energy resolution to SANS*, *Nucl. Instrum. Meth.* **A 654** (2011) 394.

[34] W. Häussler, U. Schmidt, G. Ehlers and F. Mezei, *Neutron resonance spin echo using spin echo correction coils*, *Chem. Phys.* **292** (2003) 501.

[35] H. Hayashida, M. Hino, M. Kitaguchi, Y. Kawabata and N. Achiwa, *A study of resolution function on a MIEZE spectrometer*, *Meas. Sci. Technol.* **19** (2008) 034006.

[36] N. Martin, *On the resolution of a MIEZE spectrometer*, *Nucl. Instrum. Meth.* **A 882** (2018) 11.

[37] J.K. Jochum, A. Wendl, T. Keller and C. Franz, *Neutron MIEZE spectroscopy with focal length tuning*, *Meas. Sci. Technol.* **31** (2019) 035902.

[38] M. Hino et al., *A test of MIEZE-reflectometer for study of surface and interface*, *Physica* **B 385–386** (2006) 1125.

2020 JINST 15 P04007